

MORPHOLOGICAL CHARACTERISTICS OF RETAINED AUSTENITE IN 0.362C–1.38Si–1.24Mn STEEL PROCESSED BY ONE-STEP QUENCHING AND PARTITIONING

H. R. Ghazvinloo, A. Honarbakhsh-Raouf,
and E. Borhani

The microstructure and morphology of retained austenite are effective parameters in the mechanism of plasticity enhancement in quenching and partitioning steels. This study focused on the identification of morphological features of retained austenite through scanning electron microscopy, field emission-scanning electron microscopy, electron backscatter diffractometry, and transmission electron microscopy in a one-step quenched and partitioned C–Mn–Si steel. Retained austenite of different sizes and shapes (island-like and film-like) and martensite with lath-type morphology were observed at all partitioning times. Cementite-carbide (Fe_3C) precipitates with a dominant spherical shape and average submicron size were also characterized in samples that had been partitioned for longer times.

Keywords: quenching and partitioning, retained austenite, morphology.

Introduction. In 2003, Speer et al. [1] first proposed an approach, which was termed the quenching and partitioning (Q&P) process, to exploit novel martensitic steels that contain retained austenite (Q&P steel), based on the fact that carbon can diffuse from supersaturated martensite into neighboring untransformed austenite and stabilize it to room temperature [2]. The Q&P process consists of [3]: (1) a partial or full austenitizing heat treatment, (2) a first quench (quenching step) to a temperature below the martensite-start (M_s) temperature but above the martensite-finish (M_f) temperature to form a mixture of martensite and untransformed austenite, (3) an isothermal treatment (partitioning step) at the same temperature (one-step treatment) or at a higher temperature (two-step treatment), and (4) a final quench to room temperature. The goal of the partitioning step is to enrich the austenite present at the quench temperature with carbon via carbon depletion of the martensite laths, and to decrease its M_s temperature so that thermally stable austenite is obtained after the final quenching to room temperature [4]. Therefore, final microstructures in the Q&P process contain martensite and carbon-enriched retained austenite. Martensite acts as a strengthening phase, whereas retained austenite contributes significantly to the ductility. To date, two opinions for plasticity enhancement via the retained austenite have been described. Interlath film-like austenite can impede crack generation and propagation and improve toughness [5]. Furthermore, interlath and island-like austenite can transform to martensite partially and show a “transformation-induced plasticity” effect during deformation. This transformation eliminates stress concentration and retards the occurrence of necking [6], which results in increased elongation. Few reports exist on microstructural characteristics of steels treated by Q&P [7, 8] and there is still a lack of information on the exact microstructural characterization of steels after Q&P treatment [9]. Experimental investigations of microstructural processes during Q&P can enhance our understanding of the Q&P process, and may be important for adjusting and tailoring the required mechanical properties of Q&P steels [10]. In this study, the microstructural evolutions and morphological features of retained austenite during the application of a one-step Q&P process in 0.362C–1.38Si–1.24Mn steel are reviewed and discussed.

Department of Materials Engineering, Semnan University, Semnan, Iran; e-mail: Hamid.Ghazvinloo@gmail.com.

Experimental procedure. The base material investigated in this work was 0.362C–1.38Si–1.24Mn, low-alloy steel with a chemical composition that is typical of conventional transformation-induced plasticity assisted steels. $M_s = 338.73^\circ\text{C}$ for this alloy and is determined from the empirical expression [11]

$$M_s(^{\circ}\text{C}) = 539 - 423\text{C} - 30.4\text{Mn} - 7.5\text{Si} + 30\text{Al}, \quad (1)$$

where C, Mn, Si, and Al are the elemental contents (wt.%). For one-step Q&P heat treatment, coupons (15 mm × 10 mm × 3 mm) were heated to 900°C at 5°C/sec in a furnace (model K20L1200) and held for 10 min for full austenitization, then quenched in an oil bath at 238°C (optimum quenching temperature between the martensite start and end temperatures) with a cooling rate of –220°C/sec. They were partitioned at this temperature for 10, 30, 100, 700, and 1000 sec, and then water-quenched to room temperature. After the heat treatments, the treated samples were ground and polished mechanically and then etched with 2% Nital for 6–8 sec. Microstructural examinations of the treated samples were conducted using a JEOL (JXA-840, operating at 15 and 25 kV) scanning electron microscope (SEM) and HITACHI (S-4160, operating at 30 kV) field emission-scanning electron microscope (FE-SEM). To study in detail the microstructural components of this material, one sample (quenched and partitioned at 238°C for 1000 sec) was prepared metallographically for electron backscatter diffraction (EBSD) examination and transmission electron microscopy (TEM). For the TEM and EBSD microstructure examination, the sample was thinned to ~70 μm by abrasion with SiC papers and then electro-polished in a twin-jet machine using 10% perchloric acid and 90% methanol at 20 V. A JEOL high-resolution analytical TEM operating at 200 kV and an EBSD PHILIPS machine were used.

Results and discussion. SEM micrographs of the samples quenched and partitioned at 238°C for 10, 30, 100, 700, and 1000 sec are shown in Fig. 1.

Figure 1 shows the introduction of carbon-enriched retained austenite phase into the martensitic matrix structure. The martensite with lath-type morphology is surrounded by retained austenite, and the general feature of the lath-like martensite configuration does not change much even in the sample that was treated for a longer time. The retained austenite with different sizes and with two types of morphological structures is observed at all investigated partitioning times. One has an island-like shape and is distributed mainly along the grain boundary, and a few are distributed within the martensite matrix; The other has a film-like shape and is distributed between martensite laths [12, 13]. The thicker austenitic films and many austenitic islands that are larger than a micrometer in microstructure are visible in the microstructure of samples partitioned for 10 sec. An increase in partitioning time from 30 to 100 sec led to more austenitic films with a greater thickness and elongation in the microstructure than those for a partitioning time of 30 sec. A decrease in thickness and elongation of the austenitic films occurs in samples that were partitioned for 700 sec and retained for a partitioning time of 1000 sec. Cementite-carbide (Fe_3C) precipitates within the martensite laths were also characterized in samples that were quenched and partitioned at 238°C for longer partitioning times (700 and 1000 sec) and the dominant shape was spherical with a submicron size. The partitioning time must be sufficiently long to yield considerable carbon partitioning but must also be restricted, because the risk of carbide formation as a result of the initial martensite tempering process also increases with time [14]. Carbide precipitation acts as a carbon sink, which makes carbon unavailable for austenite stabilization and therefore reduces the capacity for partitioning of carbon into austenite [14, 15]. The base material microstructure that was quenched and partitioned at 238°C for 100 sec was examined in FE-SEM micrographs (Fig. 2). The distribution of retained austenite and a dimensional analysis of this phase with different morphology, including the thickness and length of the austenitic film and the diameter of the austenitic block, are shown. The submicron cementite-carbide microstructure precipitated within the initial martensite laths is visible at a higher magnification in Fig. 3.

Because of the SEM resolution limitations, the fine sample microstructure cannot be characterized precisely [13]. Therefore, identification of different phases in the sample that was quenched and partitioned at 238°C for 1000 sec was carried out by TEM. The TEM bright-field micrograph in Fig. 4 confirms the stabilization and austenite retention in this alloy via the Q&P process. Retained austenite appears as thick films distributed between lath martensite structures. High-density dislocation tangles exist in the lath martensite structures. Dislocation strengthening of the martensite is one of the important strengthening mechanisms in Q&P steels. The dislocation densities (ρ) of the final microstructure in samples quenched and partitioned at 238°C for 10, 30, 100, 700, and 1000 sec were approximately $31.74 \cdot 10^{10}$, $15.06 \cdot 10^{10}$, $15.03 \cdot 10^{10}$, $11.25 \cdot 10^{10}$, and $6.42 \cdot 10^{10}$ cm/cm³,

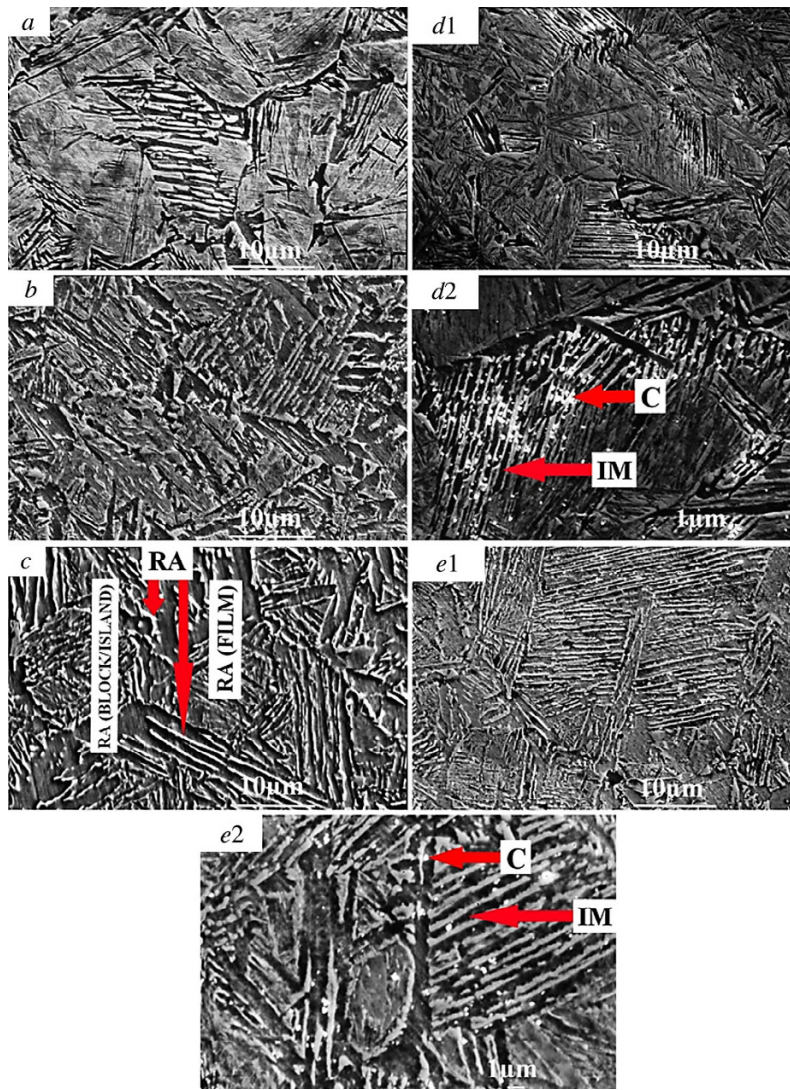


Fig. 1. SEM micrographs of treated specimens: fully austenitized at 900°C, quenched to 238°C, partitioned at 238°C for (a) 10, (b) 30, (c) 100, (d) 700, and (e) 1000 sec, and water-quenched to room temperature (C: carbide, IM: initial martensite, RA: retained austenite).

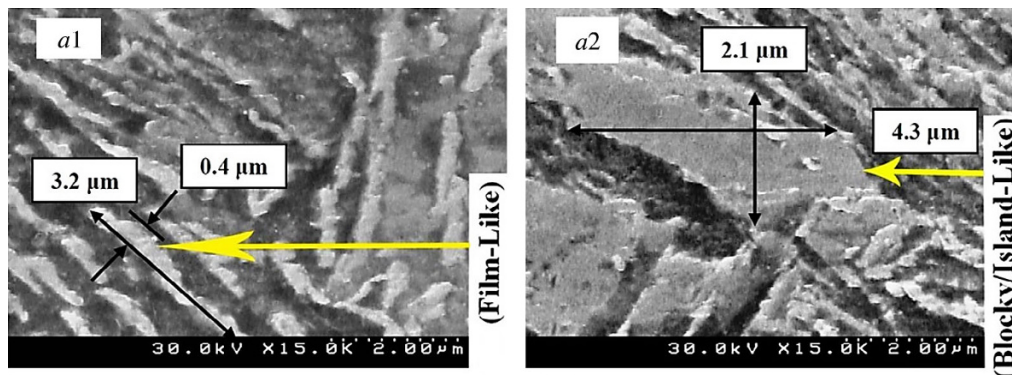


Fig. 2. FE-SEM micrographs of treated specimens: fully austenitized at 900°C, quenched to 238°C, partitioned at 238°C for 100 sec, and water-quenched to room temperature (*a1*: film-like shape; *a2*: island/blocky-like shape).

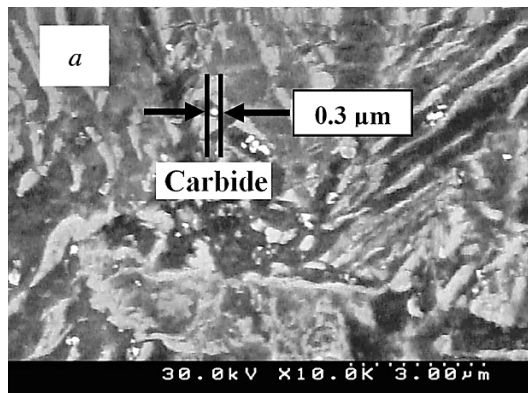


Fig. 3. FE-SEM micrograph of treated specimens: fully austenitized at 900°C, quenched to 238°C, partitioned at 238°C for 1000 sec, and water-quenched to room temperature.

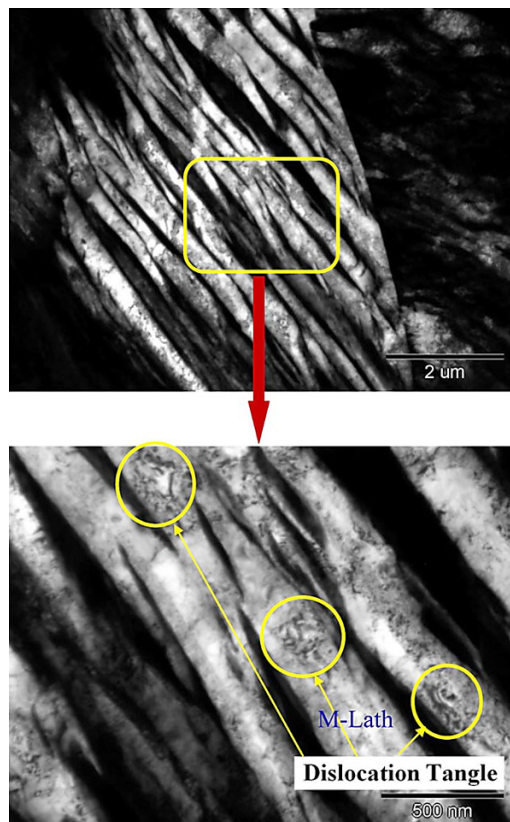


Fig. 4. TEM micrograph of treated specimens: fully austenitized at 900°C, quenched to 238°C, partitioned at 238°C for 1000 sec, and water-quenched to room temperature.

respectively, as estimated from XRD measurements on a Bruker D8 diffractometer using $\text{CuK}\alpha$ radiation at 35 kV and 30 mA. The detailed calculations from this technique are published elsewhere [16].

To support some of the mentioned microstructural features and to confirm the phase identification, EBSD analysis was performed on the sample that was quenched and partitioned at 238°C for 1000 sec. EBSD is a modern and highly effective

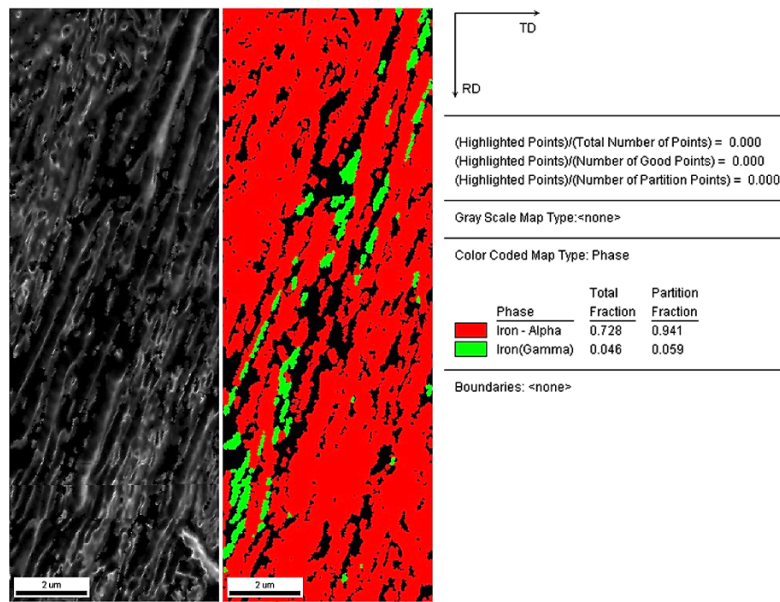


Fig. 5. Color-coded phase map obtained by EBSD for the sample quenched and partitioned at 238°C for 1000 sec.

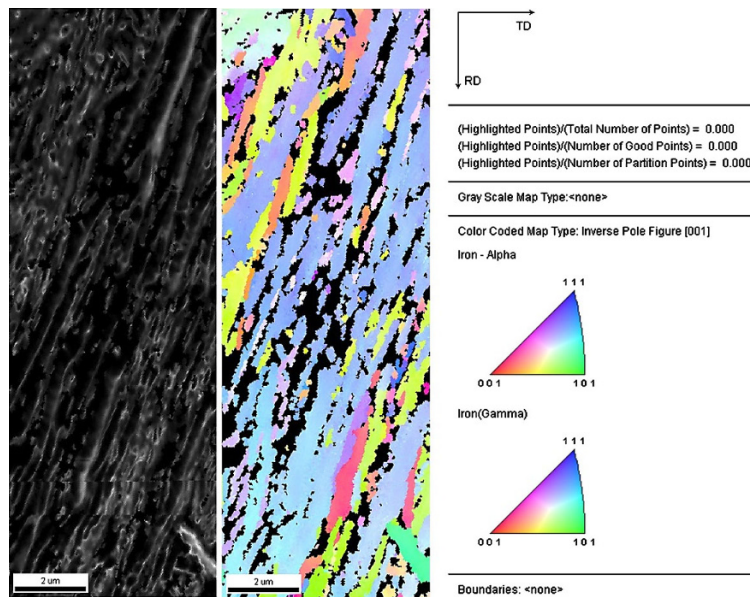


Fig. 6. Inverse pole-figure map of austenite grains obtained by EBSD for sample quenched and partitioned at 238°C for 1000 sec.

method that can be used to determine the grain orientations and identify different microstructural phases [17]. Figure 5 shows a color-coded phase map that is obtained by EBSD for the sample that was quenched and partitioned at 238°C for 1000 sec. This map confirms the different phases (α -Fe and γ -Fe) in the microstructure. The red areas correspond to bcc lattice (martensite), green areas correspond to fcc lattice (austenite), and darker bands correspond to a low band contrast. This map confirms that both kinds of retained austenite with different sizes and morphologies (island/blocky-like and film-like) exist in the

microstructure. The film-like retained austenite shows typical interlath features with a maximum length of 1.7 μm and thickness of 0.5 μm . Austenitic blocks with a maximum size of 1.2 μm are visible in this micrograph. EBSD microscopy reveals only a small area of the entire sample, which makes the quantification of a volume fraction of retained austenite inaccurate. Part of the retained austenite that could be “locked” inside the martensite laths is also not detected by the EBSD technique, because of its limited spatial resolution of 0.08 μm [7]. Consequently, the total volume fraction of retained austenite phase measured by the EBSD map (4.6%) was slightly lower than the 10.73% measured by XRD [12]. Figure 6 shows an inverse pole-figure map of the austenite grains. The colors in Fig. 6 correspond to the crystallographic orientation normal to the observed plane, as indicated in the stereographic triangle that is superimposed in Fig. 6 [13]. Austenite grains that are situated in the same region share the same crystallographic orientation. These austenite grains probably originate from a single prior austenite grain [18].

Conclusions. An overview of the phase morphology during the application of a one-step Q&P process for 0.362C–1.38Si–1.24Mn steel was presented. The most important observations are summarized as follows:

1. A microstructure that consists of a martensitic matrix and carbon-enriched retained austenite was observed for all partitioning times. The martensite phase with a lath-type morphology and surrounded by retained austenite was observed. The general feature of the lath-like martensite configuration did not change much, even in the sample that was treated for a longer time. Cementite-carbide precipitates within the martensite laths were also characterized in samples that were quenched and partitioned at 238°C for longer partitioning times (700 and 1000 sec), and the dominant shape was spherical. Carbide formation occurred as a consequence of the initial martensite tempering process. High-density dislocation tangles in the lath martensite structures were revealed by TEM.

2. Retained austenite with different sizes and two kinds of morphological structures was observed at all investigated partitioning times. Island-shaped austenite was distributed along the grain boundary mainly, with some distributed within the martensite matrix. The other austenite was film-shaped and was distributed between the martensite laths.

REFERENCES

1. J. G. Speer, D. K. Matlock, B. C. De Cooman, and J. G. Schroth, “Carbon partitioning into austenite after martensite transformation,” *Acta Mater.*, **51**, 2611 (2003).
2. L. Wang and J. G. Speer, “Quenching and partitioning steel heat treatment,” *Metall. Microstruct. Anal.*, **2**, 268 (2013).
3. M. J. Santofimia, L. Zhao, and J. Sietsma, “Microstructural evolution of a low-carbon steel during application of quenching and partitioning heat treatments after partial austenitization,” *Metall. Mater. Trans. A*, **40**, 46 (2009).
4. E. De Moor, S. Lacroix, L. Samek, et al., “Dilatometric study of the quench and partitioning process,” *3rd Int. Conf. on Advanced Structural Steels*, Gyeongju, Korea (2006).
5. B. V. N. Rao and G. Thomas, “Structure-property relations and the design of Fe–4Cr–C base structural steels for high strength and toughness,” *Metall. Trans. A*, **11**, 441 (1980).
6. X. D. Wang, B. X. Huang, Y. H. Rong, and L. Wang, “Mechanical and transformation behaviors of a C–Mn–Si–Al–Cr TRIP steel under stress,” *J. Mater. Sci. Technol.*, **22**, 625 (2006).
7. M. J. Santofimia, L. Zhao, R. Petrov, and J. Sietsma, “Characterization of the microstructure obtained by the quenching and partitioning process in a low-carbon steel,” *Mater. Charact.*, **59**, 1758 (2008).
8. M. J. Santofimia, L. Zhao, and J. Sietsma, “Microstructural evolution of a low-carbon steel during application of quenching and partitioning heat treatments after partial austenitization,” *Metall. Mater. Trans. A*, **40**, 46 (2009).
9. M. J. Santofimia, L. Zhao, R. Petrov, and J. Sietsma, “Characterization of the microstructure obtained by the quenching and partitioning process in a low-carbon steel,” *Mater. Charact.*, **59**, 1758 (2008).
10. H. Y. Li, X. W. Lu, X. C. Wu, et al., “Bainitic transformation during the two-step quenching and partitioning process in a medium carbon steel containing silicon,” *Mater. Sci. Eng. A*, **527**, 6255 (2010).
11. J. Mahieu, J. Maki, B. C. De Cooman, and S. Claessens, “Phase transformation and mechanical properties of Si-free CMnAl transformation-induced plasticity-aided steel,” *Metall. Mater. Trans. A*, **33**, 2573 (2002).

12. H. R. Ghazvinloo and A. Honarbakhsh-Raouf, "Effect of partitioning time on microstructural evolution of C-Mn-Si steel in one-step quenching and partitioning process," *J. Mater. Environ. Sci.*, **6**, 22 (2015).
13. X. D. Wang, Z. H. Guo, and Y. H. Rong, "Mechanism exploration of an ultrahigh strength steel by quenching–partitioning–tempering process," *Mater. Sci. Eng. A*, **529**, 35 (2011).
14. M. J. Santofimia, L. Zhao, and J. Sietsma, "Overview of mechanisms involved during the quenching and partitioning process in steels," *Metall. Mater. Trans. A*, **42**, 3620 (2011).
15. E. De Moor, S. Lacroix, A. J. Clarke, et al., "Effect of retained austenite stabilized via quench and partitioning on the strain hardening of martensitic steels," *Metall. Mater. Trans. A*, **39**, 2586 (2008).
16. H. R. Ghazvinloo, A. Honarbakhsh-Raouf, and A. R. Kiani Rashid, "Mechanical properties of a high Si and Mn steel heat treated by one-step quenching and partitioning," *Metallurgist*, **59**, 90 (2015).
17. E. Soppa, D. Willer, and D. Kuppler, "EBSD- and TEM-investigations of microstructure in the austenitic steel X6CrNiNb18-10 under cyclic loading," *38th MPA-Seminar*, Oct. 1–2, 2012, Stuttgart.
18. M. J. Santofimia, L. Zhao, R. Petrov, et al., "Microstructural development during the quenching and partitioning process in a newly designed low-carbon steel," *Acta Mater.*, **59**, 6059 (2011).